Available online at www.sciencedirect.com
SCIENCE DIRECT®
Biochemical and Biophysical Research Communications 327 (2005) 183–191
BBRC
www.elsevier.com/locate/ybbrc

Proteomic analysis revealed a novel synaptic proline-rich membrane protein (PRR7) associated with PSD-95 and NMDA receptor

Yasunobu Murata[a], Tomoko Doi[a], Hisaaki Taniguchi[b,c], Yoshinori Fujiyoshi[a,*]

[a] *Department of Biophysics, Graduate School of Science, Kyoto University, Oiwake, Kitashirakawa, Sakyo-ku, Kyoto 606-8502, Japan*
[b] *Institute for Enzyme Research, The University of Tokushima, Tokushima 770-8503, Japan*
[c] *Harima Institute at SPring-8, RIKEN, Mikazuki, Sayo, Hyogo 679-5148, Japan*

Received 17 November 2004
Available online 9 December 2004

Abstract

Proteomic analyses have revealed a novel synaptic proline-rich membrane protein: PRR7 (proline rich 7), in the postsynaptic density (PSD) fraction of rat forebrain. PRR7 is 269 amino acid residues long, and displays a unique architecture, composed of a very short N-terminal extracellular region, a single membrane spanning domain, and a cytoplasmic domain possessing a proline-rich sequence and a C-terminal type-1 PDZ binding motif. A fraction of PRR7 accumulates in spines along with synapse maturation, and colocalizes with PSD-95 in a punctate pattern in rat hippocampal neural cultures. Immunoprecipitation and GST pull-down assays demonstrated that PRR7 binds to the third PDZ domain of PSD-95. In addition, the NMDA receptor subunits, NR1 and NR2B, specifically co-immunoprecipitated with PRR7. These results suggest that PRR7 is involved in modulating neural activities via interactions with the NMDA receptor and PSD-95, and PSD core formation.

Keywords: Postsynaptic density; Mass spectrometry; PDZ domain binding motif; Proline-rich motif; Hippocampal neuron

The postsynaptic density (PSD) is a thick and dense structure, observed in the excitatory postsynaptic membrane, which involves various kinds of proteins, such as ion channel, scaffolding, cytoskeletal, and signaling proteins. Studies of the molecular components of the PSD over the last two decades have revealed the highly organized protein networks in the synapse and their role in synaptic transmission [1,2]. The formation of the super-molecular complex beneath the postsynaptic membranes, and the activity-dependent alternations in its composition, such as the recycling of AMPA receptors and ubiquitin-mediated protein turnover, facilitate rapid and accurate synaptic transmission and confer synaptic plasticity [3,4].

Recent advances in proteomic techniques and their applications to brain science have revealed novel proteins that participate in specific neural activities. The PSD is a detergent-resistant and rigid structure, and thus it can be isolated as a Triton X-100 insoluble fraction by a series of sucrose gradient sedimentations. This biochemically isolated PSD fraction has been studied by proteomic analyses, and the involvement of more than 300 proteins in the PSD fraction has been described [5–8]. Characterization of these novel PSD proteins is important and is required not only for the elucidation of their functions in brain activities, but also for the expansion of our understanding of the postsynaptic molecular organization responsible for complex neural transmission and modulation.

We also conducted a proteomic analysis of the sucrose density gradient-isolated PSD fraction and

* Corresponding author. Fax: +81 75 753 4218.
E-mail address: yoshi@em.biophus.kyoto-u.ac.jp (Y. Fujiyoshi).

0006-291X/$ - see front matter © 2004 Elsevier Inc. All rights reserved.
doi:10.1016/j.bbrc.2004.11.154

identified more than 300 proteins, among which approximately 30 functionally unknown proteins were included, together with most of the known PSD proteins (unpublished data). The functions of most of the novel PSD proteins cannot be estimated by using the current references and sequence information. However, their localization in the PSD fraction suggests their involvement in synaptic activity. In this present study, we focused on one novel protein, PRR7 (proline rich 7), approved by the Mouse Genomic Nomenclature Committee, on the basis of a root symbol for proline-rich proteins. This protein shares no clear homology with any other known proteins. The deduced protein sequences of PRR7 in mouse and rat are 269 amino acid residues long, consisting of a very short N-terminal extracellular domain, a single membrane spanning domain, and a cytoplasmic domain containing a proline-rich sequence and a PDZ binding motif. This novel secondary structure hampers prediction of its function. To explore its function, we raised an antibody against PRR7, and studied its localization and interacting partners in hippocampal neurons and in the brain.

Materials and methods

Isolation of the PSD fraction by subcellular fractionation. The PSD fractions were prepared as previously described [9,10], with slight modifications. All experimental steps were performed at 4 °C or on ice, and all of the *g* values are the average centrifugation forces. The forebrains of Wistar six-week-old rats were homogenized in 0.32 M sucrose, 1 mM $MgCl_2$, 0.5 mM $CaCl_2$, and 1 mM $NaHCO_3$, and then were centrifuged at 710*g* for 10 min to remove the cell debris and nuclei. The obtained supernatant (S1: low-speed supernatant) was centrifuged at 12,000*g* for 15 min, and the resulting supernatant (S2: high-speed supernatant) was removed. The remaining pellet (P2: crude membrane fraction) was homogenized in the same buffer, applied to a discontinuous sucrose gradient consisting of 1.0 and 1.4 M sucrose in 1 mM $NaHCO_3$, and centrifuged at 82,500*g* for 65 min. The synaptosome fraction was isolated from the interface between the 1.0 and 1.4 M sucrose layers. The fraction containing myelin and light membrane was obtained from above the 1.0 M sucrose layer, and the mitochondria were sedimented in the pellet. The synaptosome fraction was subjected to osmotic shock by an incubation in 1 mM $NaHCO_3$ for 20 min, solubilized in 0.5% TX-100, 0.16 M sucrose, and 6 mM Tris–HCl (pH 8.1) for 15 min, and then centrifuged at 82,800*g* for 20 min. The obtained pellet was homogenized in 0.32 M sucrose in 1 mM $NaHCO_3$, applied to a second sucrose step gradient consisting of 1.0, 1.5, and 2.1 M sucrose, and centrifuged at 201,800*g* for 315 min. The fraction between the 1.5 and 2.1 M sucrose layers was collected, further solubilized in 0.5% Triton X-100 and 75 mM KCl for 15 min, and applied to a final sucrose step gradient consisting of 1.5 and 2.1 M sucrose, which was centrifuged at 201,800*g* for 315 min. The PSD fraction was obtained from the interface between the 1.5 and 2.1 M sucrose layers, and was suspended in 5 mM Hepes/KOH (pH 7.4), 20% glycerol.

1D-gel SDS–PAGE, preparation of LC/MS/MS sample, and nano LC/MS analysis. An aliquot of the PSD fraction, containing 50 μg protein, was dissolved in SDS sample buffer (62.5 mM Tris–HCl (pH 6.8), 2% SDS, 5 mM EDTA, 10% glycerol, and 20 mM DTT) and subjected to 1D-gel SDS–9% PAGE, using a gel with 16 cm length and 1.0 mm thickness. The gels were visualized with Coomassie brilliant blue (CBB) or mass (MS)-compatible silver staining [11].

The entire lane of the PSD fraction was cut equally into 93 gel slices, regardless of their staining pattern. The obtained gel slices were subjected to in-gel tryptic digestion, as described previously [11,12]. Digested peptides were extracted twice by incubations with 5% formic acid in 50% acetonitrile at room temperature for 30 min. The extracted peptides were dried out completely and reconstituted in 0.1% formic acid. The samples were stored at −80 °C until LC/MS/MS analysis.

Column injection and chromatographic separation of the peptide mixture were carried out by the CAPLC system (Waters). The nano LC column (PepMap C18, 75 μm × 150 mm, LC Packings) was eluted with a linear gradient of acetonitrile in the presence of 0.1% formic acid, and the column eluate was directly injected into the nano-electrospray interface. The quadrupole time-of-flight mass spectrometer (Q-Tof-2, Micromass) was operated in the survey scan mode by the MassLynx Software. The acquired MS/MS spectra were processed into text-formatted files, and the database search was conducted using the Mascot search engine (Matrix Science).

Sequence (informatic) analysis. The homology search was performed with the BLAST servers of the National Center for Biotechnology Information. The membrane topology was predicted by TMHMM ver2.0, on the WWW Prediction servers of the Center for Biological Sequence Analysis, and by TMPred of the Swiss Institute for Bioinformatics. The multiple sequence alignment was performed by ClustalW on the Web server of the European Bioinformatics Institute.

DNA constructs and recombinant proteins. The coding region of PRR7 was acquired from the mouse brain full-length cDNA library (Clontech) by using an Advantage GC 2 PCR kit (Stratagene), according to the supplier's recommendations. The following primers were used: forward primer: 5′-ATGGTGATGTCCCAGGGCACC TAC-3′, reverse primer: 5′-TACGGCTGTAGTCCTCCCGAACAA-3′. The acquired gene was 810 bp long and corresponded completely to the predicted cDNA sequence. The PRR7 cDNA was subcloned into the pCA-pA mammalian expression vector under the chicken β-actin promoter [13].

The construction of the GST-fused PDZ1 and PDZ2 domains of PSD-95 was described previously [14]. The PDZ3 and SH3-GK domains of PSD-95 were subcloned into the pGEX-4T3 vector (Amersham Biosciences) in a similar manner, and all constructs were verified by DNA sequencing.

Antibodies. The PRR7 antibody was generated by immunizing rabbits with a synthetic peptide, PRPWSYPRQAESDMSK, corresponding to residues 129–144 in mouse and rat PRR7, and residues 134–149 in the human form, respectively. The obtained antisera were affinity-purified on agarose columns conjugated with the antigen peptide.

The following antibodies were used at the indicated concentrations: for immunoblotting, mouse anti-PSD-95 at 0.1 μg/ml (K28/43, Upstate Biotechnology), mouse anti-β actin at 1:5000 (Sigma), rabbit anti-PRR7 at 1 μg/ml, horseradish peroxidase-conjugated anti-rabbit or anti-mouse at 1:5000 (Qiagen); for immunocytochemistry, mouse anti-PSD95 at 1:300 (7E3, Affinity BioReagents), rabbit polyclonal anti-PRR7 at 2 μg/ml, and Alexa 488 or 594-conjugated goat anti-mouse or anti-rabbit at 1:300 (Molecular Probes).

COS-1 cell culture and transfection. COS-1 cells were cultured in Dulbecco's modified Eagle's medium (Sigma), supplemented with 10% fetal bovine serum and penicillin/streptomycin, at 37 °C under 5% CO_2. Transfection was performed by lipofection using the Effectene reagent (Qiagen), according to the supplier's recommendations. After 48 h of transfection, the cells were collected from a 10 cm dish, suspended in 500 μl ice-cold RIPA Buffer (50 mM Tris–HCl (pH 7.5), 150 mM NaCl, 1% Nonidet P-40, 0.5% deoxycholate, and 0.1% SDS) containing a protease inhibitor cocktail (Roche), and then incubated on ice for 30 min. After centrifugation at 10,000*g* for 10 min, the supernatants thus obtained were used for further experiments.

Immunoblotting. For immunoblotting analyses, the proteins were resolved on 7.5% and 12.5% polyacrylamide gels (Daiichi Pure Chemicals) and transferred to a PVDF membrane (Bio-Rad) using a

semi-dry transblotter (Nihon Eido). The membrane was incubated in blocking buffer (5% skim milk, 50 mM Tris–HCl (pH 7.5), 150 mM NaCl, and 0.1% Tween 20) at room temperature for 1 h, and then incubated with a primary antibody diluted in blocking buffer at 4 °C overnight. The membrane was rinsed with TBST (50 mM Tris–HCl (pH 7.5), 150 mM NaCl, and 0.1% Tween 20), and incubated with an HRP-conjugated secondary antibody diluted in TBST at room temperature for 1 h. Immunoreactive proteins were detected by using ECL plus (Amersham Biosciences) and Image Master (Amersham Biosciences).

Extraction of PRR7 from rat brain crude membrane. The brain crude membrane fraction (P2 fraction, 5 mg protein) was suspended in 500 μl of extraction buffer, containing the indicated detergent, in 50 mM Tris–HCl (pH 7.5), 150 mM NaCl, and 10 mM EDTA. The DOC buffer consisted of 2% sodium deoxycholate, 50 mM Tris–HCl (pH 9.5), and 50 mM sodium fluoride. The suspensions were gently rotated at 4 °C for 1 h and then were centrifuged at 13,000*g* for 10 min. The supernatants were collected, and the remaining pellets were suspended in 500 μl SDS sample buffer. Ten microliters of each sample was analyzed by immunoblotting.

Immunoprecipitation of the PRR7 complex from rat brain extract. The brain crude membrane fraction (P2 fraction, 3 mg protein) was solubilized in 500 μl DOC buffer (2% sodium deoxycholate, 50 mM Tris–HCl (pH 9.5), 50 mM sodium fluoride, and protease inhibitors) at 4 °C for 1 h and then was centrifuged at 13,000*g* for 10 min. The supernatants were mixed with 500 μl cell lysate, prepared from COS-1 cells transfected with or without the PRR7 expression plasmid, as described above.

The mixtures were incubated with 5 μg of affinity-purified anti-PRR7 antibody at 4 °C for 3 h, and 15 μl of Protein-G conjugated magnetic beads (Dynabeads ProteinG, Dynal) was added to each tube. After a further incubation for 45 min, the beads were washed three times with ice-cold wash buffer (0.1% TX-100, 50 mM Tris–HCl (pH 7.4), 150 mM NaCl, 10 mM EDTA, and protease inhibitors). The bound proteins were eluted by boiling with 20 μl SDS sample buffer for 5 min, fractionated by SDS–8% PAGE (8 cm length, 1 mm thickness), and visualized by MS-compatible silver staining. Proteins of the same eluates were also analyzed by immunoblotting.

GST pull-down assay. The GST-fused proteins were expressed in the *Escherichia coli* BL21 strain. The cells were harvested and lysed in CelLytic B Bacterial Cell Lysis Reagent (Sigma), containing protease inhibitors, at room temperature for 10 min. After centrifugation at 13,000*g* for 10 min, the supernatants were collected and used for the following experiments.

The bacterial lysates (10 mg protein) and COS-1 cell lysates from cells expressing PRR7, prepared from a 100 mm dish, were mixed, scaled up to 1 ml with ice-cold RIPA buffer, and then incubated with a 20 μl bed volume of glutathione–Sepharose beads (Amersham Biosciences) at 4 °C for 1 h. The beads were washed with ice-cold RIPA buffer three times, and then the bound proteins were eluted with RIPA buffer containing 50 mM glutathione and analyzed by immunoblotting.

Hippocampal neural cell cultures. Rat hippocampal neurons were prepared from embryonic day 18 Wistar rats, as described [15,16]. The hippocampal neurons were isolated by trypsin treatment and trituration, and then were plated on poly-L-lysine-coated coverslips, at a density of 3000 cells/cm^2. The neural cultures were maintained in Neurobasal medium (Invitrogen) supplemented with 1/50 volume of B-27 (Invitrogen) and 200 mM glutamate.

Immunostaining of hippocampal neural cultures. The hippocampal neurons on the coverslips were washed with Hanks' balanced salt solution (Sigma), containing 1 mM $MgCl_2$ and $CaCl_2$, and fixed with ice-cold methanol at −20 °C for 20 min. After a rinse with PBS, the samples were permeabilized by 0.25% Triton X-100 in PBS at 4 °C for 10 min, and blocked by an incubation with PBS containing 5% skim milk and 5% normal goat serum at 37 °C for 30 min. The primary antibodies were added to the blocking buffer, and the mixtures were incubated at room temperature for 1 h. The samples were then washed with PBS and labeled with Alexa 488 or 594-conjugated secondary antibodies, diluted in the blocking buffer at room temperature for 30 min. Finally, the coverslips were washed with PBS and mounted on the slides, using the FluorSave reagent (Calbiochem).

Images were obtained with a Zeiss LSM 510 laser scanning confocal microscope system through a 63 × (1.4NA) objective lens. Images were prepared for printing with the Adobe Photoshop software.

Results and discussions

Preparation of the PSD fraction

The PSD fraction was prepared, based on the classical procedure described by Cohen and co-workers [9,10], which involves two rounds of solubilization of synaptosomal membrane fraction with Triton X-100 and subsequent sucrose density gradient centrifugation. Four milligrams of PSD fraction was obtained from 15 g of the forebrains of six-week-old rats. The PSD proteins were resolved by one-dimensional SDS–PAGE (Fig. 1A), and then the single lane was cut into 93 equal gel slices, as shown on the right side. The proteins contained in each gel slice were analyzed by LC/MS/MS after in-gel tryptic digestion.

Identification of PRR7 in the rat brain PSD fraction

Our proteomic analysis revealed that approximately 300 proteins were contained in the PSD fraction, including about 30 functionally unknown proteins (unpublished data). Here, we focused on one novel protein with an unknown function, PRR7. PRR7 was identified as a 35–40 kDa human hypothetical protein MGC10772 (NCBI Accession No. GI21361937). In the public database, MGC10772 was initially assigned as a full-length human cDNA sequence by the Mammalian Genome Collection Project of National Institute of Health [17,18]. As shown in Fig. 1B, six unique peptides observed by the MS/MS analysis matched the predicted amino acid sequence of PRR7, and the sequence coverage by the six peptides was 21%.

PRR7 shows no clear homology to other known proteins, and the orthologous genes found in the current database are restricted to human, mouse, and rat. The coding regions of PRR7 gene are 825 bp long in human and 810 bp long in mouse and rat. PRR7 was predicted to consist of two protein-coding exons, and no other possible splicing products were found by the informatic analysis. Furthermore, the isolated cDNA of the mouse PRR7 was identical to the predicted cDNA sequence.

Properties of the PRR7 amino acid sequence

The deduced PRR7 amino acid sequences from the human (274 amino acids), and mouse and rat (269 amino acids) forms, are shown in Fig. 1C. These orthologs

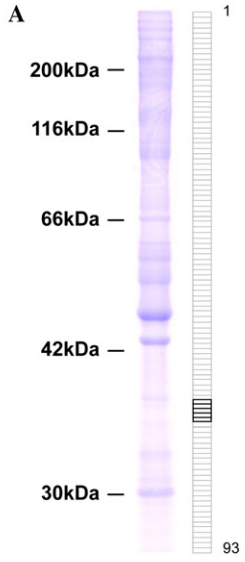

B

Position	Peptide Sequence	Mascot Score
179-187	KIVTPFLSR	46
180-187	IVTPFLSR	32
194-208	QEQPPPSYKPLFLDR	47
239-251	VFPSWTDSELSSR	51
252-260	EPLEHGAWR	47
261-270	LPVSIPLFGR	72

C

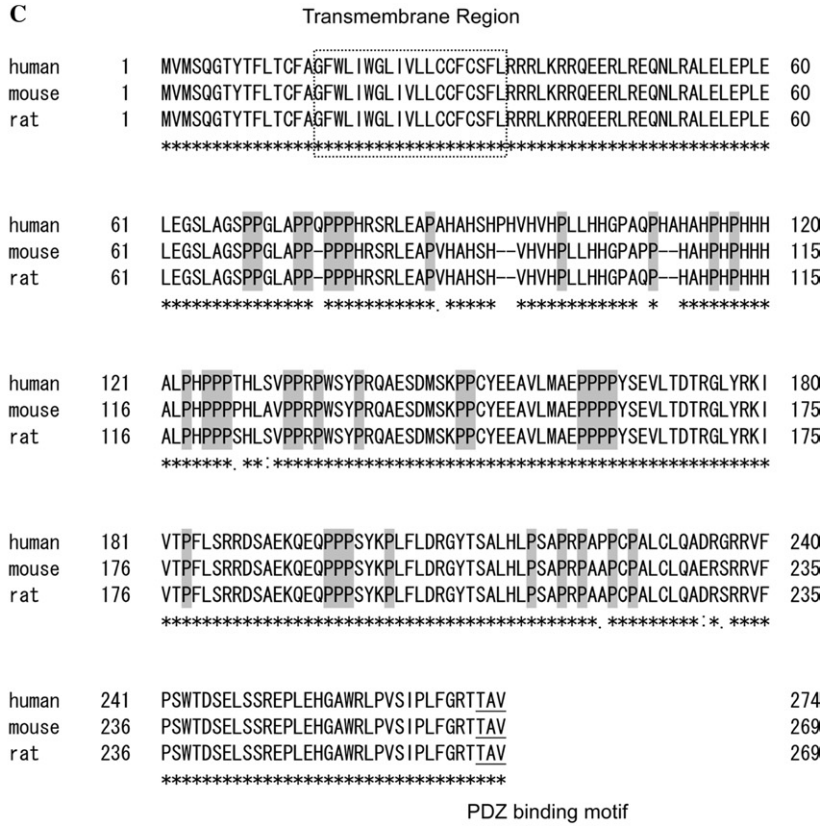

Fig. 1. Identification of PRR7 from the rat brain PSD fraction. (A) 1D SDS–PAGE gel of the PSD fraction. The rat forebrain PSD fraction (50 μg) was subjected to one-dimensional 9% SDS–PAGE (16 cm by length, 1.0 mm by thick). The CBB-stained gel was sliced to give 93 equal gel pieces with a width of 1.7 mm. PRR7 was identified at approximately 35–40 kDa (boxed regions). The molecular weights of the standard proteins are shown on the left side. Schematic 93 equal gel slices of a single lane are shown on the right side. (B) The peptides used to identify PRR7. Six unique peptides observed by LC/MC/MS analysis were used to identify PRR7. The starting and ending positions, the amino acid sequence, and the Mascot identification score of each peptide are shown in the table. The sequence coverage of LC/MC/MS analysis was 21%. (C) Amino acid sequence of PRR7 from human, mouse, and rat. Identical amino acids are indicated with asterisks, highly similar amino acids are highlighted with colons, and low similarity amino acids are shown with dots. PRR7 is highly conserved between human, mouse, and rat. The orthologs have 94% or more identical amino acid sequences to each other. The predicted transmembrane region is boxed with a dashed line, the conserved proline residues are colored gray, and the PDZ-binding motifs are underlined.

are highly conserved and share 94% or more amino acid sequence identity with each other. An informatic analysis of the amino acid sequence of PRR7 predicted one single-spanning transmembrane domain, located near the N-terminus, with most of the polypeptides residing in the cytoplasmic domain.

In the middle of the cytoplasmic domain, proline-rich sequences are observed. The 36 conserved proline residues exist in the region of residues 65–240. This unusually high proline content is an outstanding feature of PRR7. In addition, the type I PDZ binding motif, TAV, is present at the carboxyl terminus, suggesting its interaction with scaffolding proteins.

Evaluation of the affinity-purified antibody for PRR7

The specificity of the rabbit polyclonal anti-PRR7 antibody, raised against a synthetic peptide, was confirmed by immunoblotting (Fig. 2A). A single band was detected around 37 kDa in the COS-1 cell lysate transfected with the PRR7 cDNA, consistent with the MS-identification. No other bands were detected in the control cell lysates. The observed molecular weight of PRR7 in SDS–PAGE is slightly larger than that calculated from its amino acid composition (30 kDa), probably due to its unique amino acid composition and/or unrevealed modifications such as palmitoylation or phosphorylation.

Immunoblotting of the rat brain homogenate and the PSD fraction also revealed the existence of the 37 kDa band, especially in the PSD fraction (Fig. 2B). In the brain homogenate, the 37 kDa band was very faint, suggesting the low abundance of PRR7. The minor bands in the brain homogenates appear to be due to background in the detection.

Subcellular distribution of PRR7 in the brain and its detergent insolubility

To examine the subcellular distribution of PRR7, each fraction obtained during the preparation of the

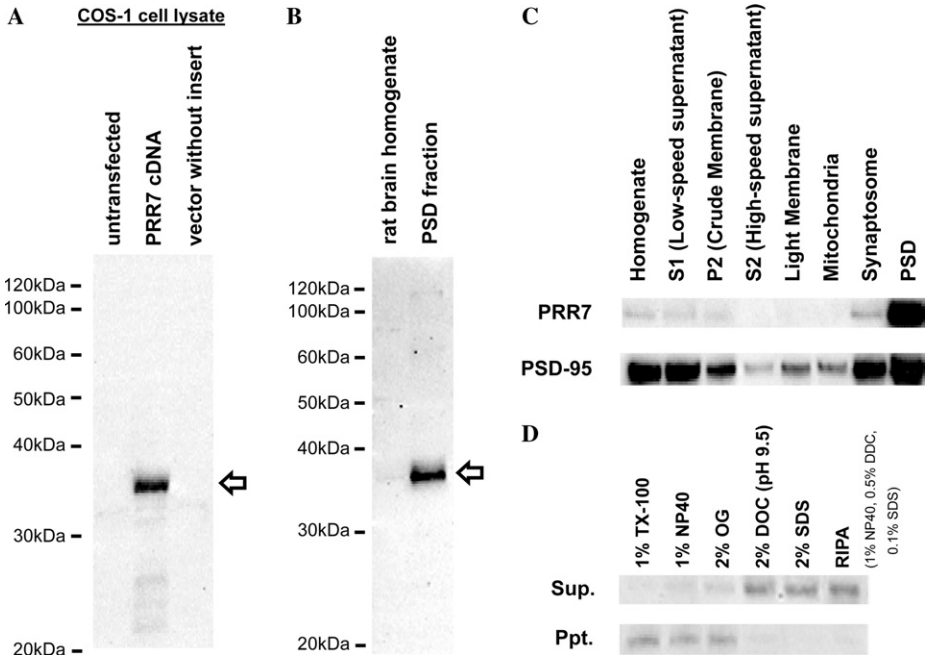

Fig. 2. Characterization of PRR7 using the specific antibody. (A) Lysates of COS-1 cells transfected with the PRR7 cDNA were analyzed by immunoblotting, using the rabbit polyclonal anti-PRR7 antibody. The lysates of cells untransfected and transfected with the pCA-pA vector without an insert were also analyzed as a control. (B) Five micrograms of rat brain homogenate and the PSD fraction was analyzed by immunoblotting, using the anti-PRR7 antibody. The molecular weights of the standard proteins are shown on the left side, and the arrows indicate the band of PRR7. (C) Subcellular distribution of PRR7 in the rat forebrain. The brain subcellular fraction was prepared as described in the Materials and methods. Five milligrams of each fraction was analyzed by immunoblotting. Another polyacrylamide gel was stained by CBB to confirm the equal loading of each fraction (data not shown). PSD-95 is shown as a control of our subcellular fractionation. (D) Solubilization of PRR7 by various detergents. The brain crude membrane fraction (P2) was solubilized with the extraction buffer containing each detergent, as indicated on the top of the panel, at 4 °C for 1 h. After centrifugation at 13,000*g* for 10 min, the obtained supernatant (Sup.) and pellet (Ppt.) fractions were analyzed by immunoblotting.

PSD fraction was analyzed by immunoblotting. As shown in Fig. 2C, PRR7 was highly concentrated in the PSD fraction. As compared to PSD-95, this extent of enrichment in the PSD fraction is remarkable, suggesting the tight association of PRR7 with the core PSD components.

In addition, PRR7 is quite detergent-insoluble, as shown in Fig. 2D. PRR7 was resistant to solubilization by NP40, TX-100, and OG (*n*-octyl-β-D-glucopyranoside), which is a typical feature of the core PSD proteins. The high detergent insolubility of PRR7 also suggests its involvement in the detergent-resistant complex, via robust protein–protein or protein–lipid interactions.

PRR7 expression pattern

We examined the regional and temporal expression of PRR7 in the rat brain. Immunoblotting of protein extracts from different regions of the rat brain showed that PRR7 expression was restricted to the cerebral cortex and especially to the hippocampus (Fig. 3A).

Immunoblot analyses of the cerebral cortex at various developmental stages showed that the expression of PRR7 was undetectable in the prenatal stage and progressively increased during maturation (Fig. 3B). Immunoblotting analyses of hippocampal homogenates also revealed the same expression pattern (data not shown). These results suggest its potential roles in synapse formation and modification in the maturation process.

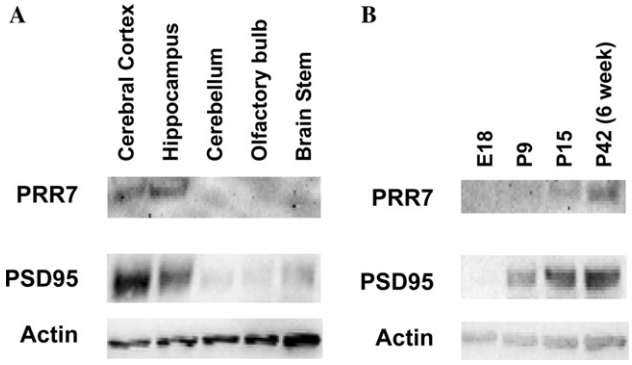

Fig. 3. Expression pattern of PRR7 in the rat brain. (A) Expression of PRR7 in different regions of the rat brain. Ten micrograms of the homogenates, prepared from different regions of six-week-old rat brains, was analyzed by immunoblotting. The brain stem mentioned here involves the diencephalons, midbrain, pons, and medulla oblongata. (B) Expression of PRR7 during rat brain development. Ten micrograms of homogenates of rat cerebral cortex, obtained at embryonic day 18 (E18), P9, P15, and P42 (6 weeks), was analyzed by immunoblotting. PSD-95 serves as a representative of postsynaptic proteins and β-actin was monitored as a loading control.

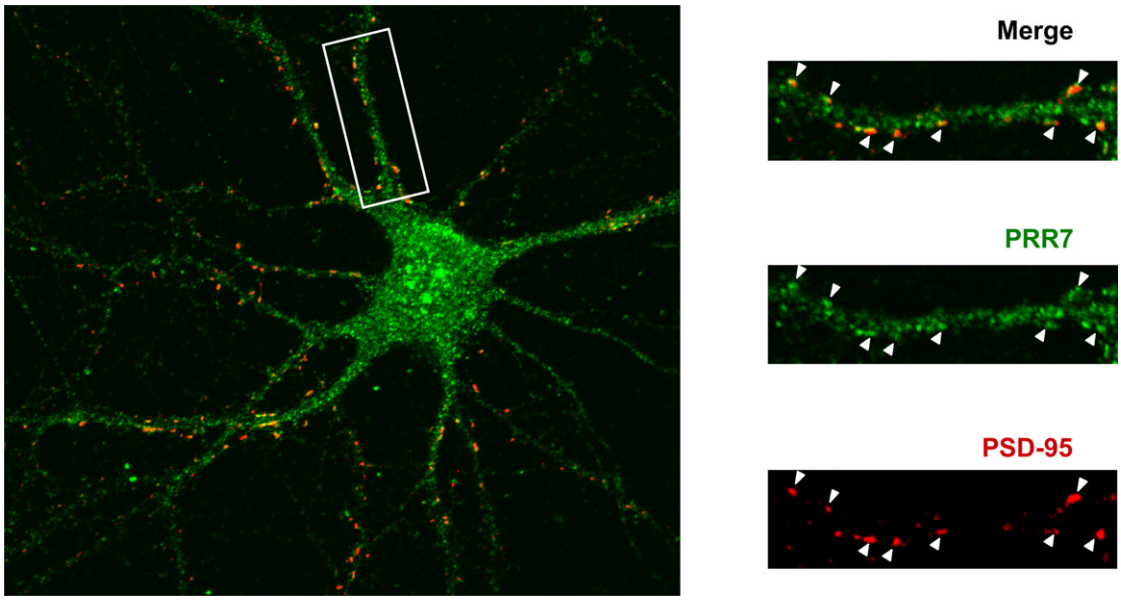

Fig. 4. Localization of PRR7 in cultured hippocampal neurons. Hippocampal neural cells, cultured for 24 days, were doubly stained with anti-PRR7 (green) and anti-PSD95 (red). Colocalization of both proteins is evident by the yellow staining in the merged picture. Magnified images of the boxed region are shown on the right side. Arrowheads indicate the significantly colocalized signals of PRR7 and PSD-95.

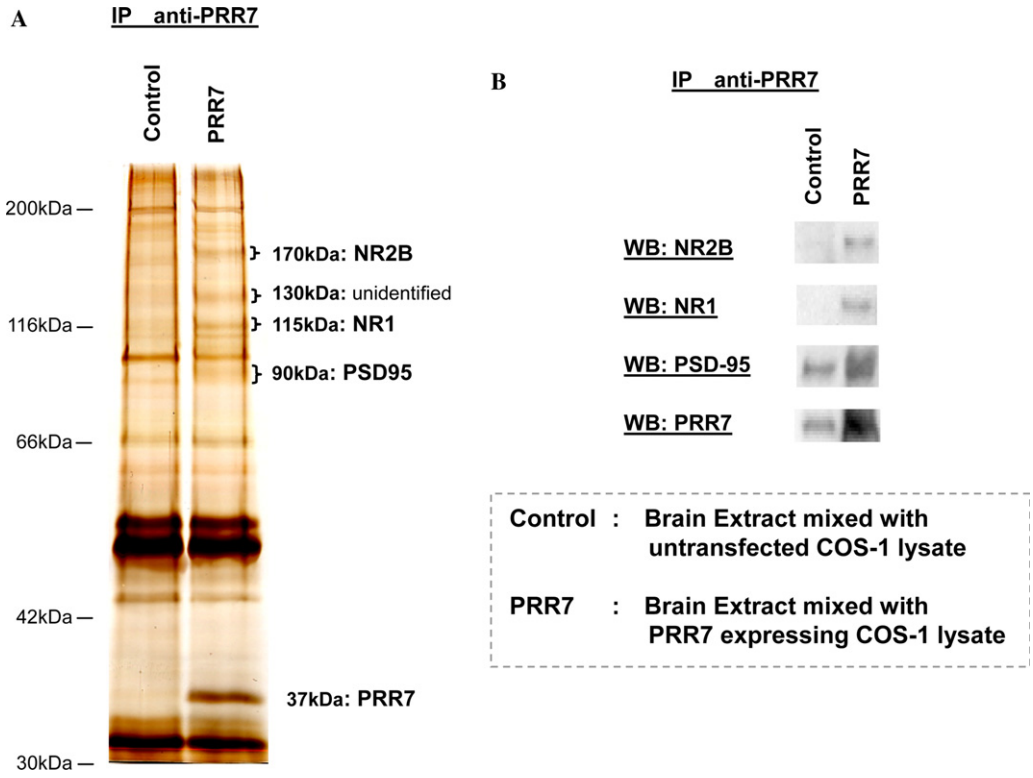

Fig. 5. Immunoprecipitation of the mixture of rat brain extract and COS-1 cells transfected with or without PRR7 cDNA. (A) Immunoprecipitates from the mixture of rat brain extracts and expressed PRR7. The rat brain extracts were mixed with lysates from COS-1 cells heterogeneously expressing PRR7 (PRR7) or untransfected cells (control), and then immunoprecipitations using anti-PRR7 antibody were conducted. The eluates were subjected to SDS–PAGE and visualized by MS-compatible silver staining. Unique bands at approximately 170, 130, and 115 kDa can be seen in the mixture with the expressed PRR7. The 90 kDa band was enriched in a PRR7 dependent manner. Mass spectrometry analyses identified NR2B at 170 kDa, NR1 at 115 kDa, and PSD-95 at 90 kDa, respectively. The protein at 130 kDa could not be identified in this study. (B) Immunoblot analysis of each precipitant. The same eluates (immunoprecipitants) were also analyzed by immunoblotting using anti-NR2B, anti-NR1, anti-PSD-95, and anti-PRR7 antibodies. These results also confirmed that these proteins were enriched in the mixture with the expressed PRR7.

Localization of PRR7 in a hippocampal primary culture

The cellular distribution of PRR7 was analyzed in a hippocampal neural culture at 24 days in vitro. Immunostaining revealed the punctate-like expression pattern of PRR7 (green), which was colocalized with a postsynaptic marker, PSD-95 (red) (Fig. 4). The signals observed in the dendrites and cell body could be attributed to a fraction of PRR7 localized in the detergent-insoluble membrane domain such as lafts, or backgrounds of nonspecific interaction by the anti-PRR7 antibody. In the earlier stages, significant signals for PRR7 were not detected, probably due to its minimal accumulation and/or lack of clustering.

Immunoprecipitation of brain extracts with anti-PRR7 antibody

To examine the function of PRR7, we purified the PRR7-associating proteins from rat brain extract by means of immunoprecipitation. The rat brain extracts were mixed with the COS-1 cell lysates containing heterologously expressed PRR7, or with the untransfected COS-1 cell lysates (control), and then were immunoprecipitated with the anti-PRR7 antibody. The immunoprecipitates were separated by SDS–PAGE and visualized by MS-compatible silver staining (Fig. 5A). Some of these bands may be nonspecific binding products, because they also appeared in the control. Nevertheless, unique proteins at 170, 130, and 115 kDa were precipitated in a PRR7-dependent manner, and the 90 kDa band shows a stronger intensity (right lane of Fig. 5A), as compared to the control sample (left lane of Fig. 5A).

Further analyses of these bands by mass spectrometry, identified NR2B at 170 kDa, NR1 at 115 kDa, and PSD-95 at 90 kDa, respectively. Proteins contained in the band at 130 kDa could not be identified in this experiment. Immunoblot analyses also confirmed the co-precipitation of these proteins with PRR7 (Fig. 5B).

It is conceivable that PSD-95 binds directly to PRR7 via its PDZ binding motif. As shown in Figs. 2 and 4, PRR7 is proved to be the core component of postsynaptic density, thus NMDA receptor may form a stable protein complex containing PRR7 and PSD-95 together with other PSD proteins, which resulted in the coprecipitation of NMDA receptor with PRR7. However, it is likely that PRR7 directly binds to the NMDAR because the enrichment of NMDAR in the coprecipitates is much more significant than that of PSD-95, and because separately solubilized NMDAR from the brain extracts and PRR7 from the COS-1 cell lysates formed coprecipitates. In addition, only a few bands including NR1 and NR2B were specifically detected in a PRR7-dependent manner, while PSD-95 interacts with many kinds of proteins.

The NMDA receptor binds directly to EphB receptor via the extracellular domain, depending upon its ligand EphrinB binding [19], and to dopamine D1 receptor [20] and RasGRF1 [21] via the cytoplasmic domain. These interactions are critical to regulate the signal transmission by the NMDA receptor. Although the cellular and neural function of PRR7 is not clear at this point, the tight association of PRR7 with NMDA receptor may play a significant role in the regulation of NMDA receptor function and its downstream signal transduction.

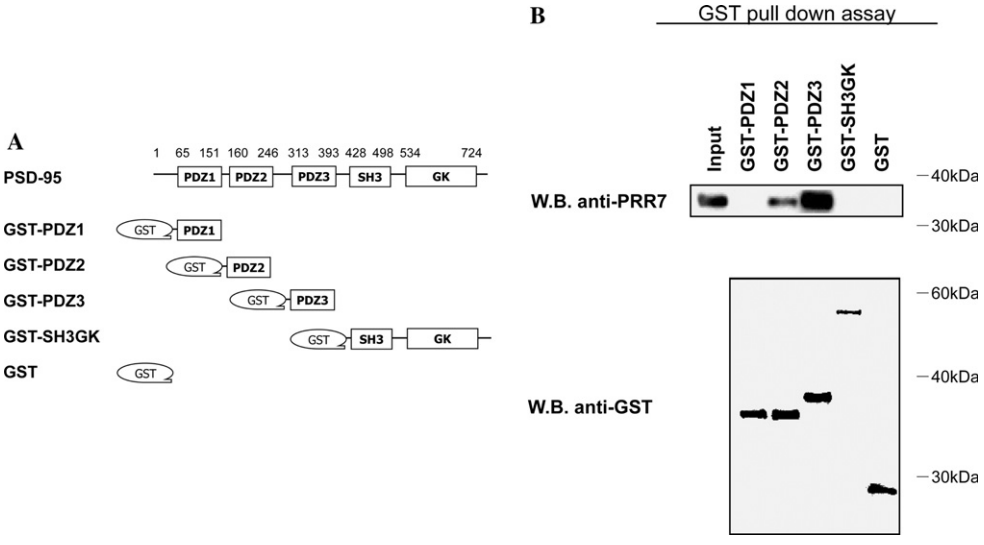

Fig. 6. A GST pull-down assay with different domains of PSD-95 and PRR7. (A) A schematic representation of the full-length PSD-95 and the GST-fusion constructs used for pull-down assays. (B) The results of the GST-pull-down assay. The COS-1 cell lysate expressing PRR7 and the bacterial lysates expressing each GST-fusion protein were mixed and then incubated with glutathione–Sepharose. The GST-fusion proteins were collected, and the bound proteins were analyzed by immunoblotting.

PRR7 binds to the PDZ3 domain of PSD-95

PSD-95 is the major binding partner of PRR7, as shown in Fig. 5. The C-terminal amino acid sequence of PRR7, TAV, is a typical PDZ binding motif (Type-1: S/T-X-V-COOH), but the identical sequence has not been shown to bind to PSD-95. Therefore, the binding ability of PRR7 to PSD-95 was examined by a pull-down assay using GST-fusion proteins. Fig. 6 demonstrated that PRR7 binds preferentially to the PDZ3 domain of PSD-95, and to lesser degree to PDZ2, but not to the PDZ1 and SH3-GK domains under the conditions employed.

Although the number of PSD-95 interacting proteins exceeds 30 [22], only a few proteins such as Citron [23], CRIPT [24], and Neuroligin [25] preferentially bind to the PDZ3 domain. Since the NMDA receptor binds to the PDZ1 and PDZ2 domains of PSD-95, the binding of PRR7 to the PDZ3 domain might play compensatory roles in the formation and regulation of the PSD structure.

Conclusion

Proteomic analysis allowed identification of PRR7, a novel proline-rich membrane protein that interacts with PSD-95 and NMDA receptor. Detection of proteins with low abundance and uncharacterized sequence, such as PRR7 is a major advantage of proteomic analysis. Further biochemical studies revealed that PRR7 was one of the core components of the postsynaptic density. The expression pattern in brain suggests its possible involvement in synaptic formation or maturation especially in the cerebrum including the hippocampus.

Since PRR7, the NMDA receptor, and PSD-95 bind to one another, PRR7 might play a role in forming a stable, rigid complex, including the PSD-95 and NMDA receptor, in the postsynaptic membrane. Furthermore, the highly conserved proline-rich sequence in PRR7 may play significant roles in protein–protein interactions. In general, proline-rich sequences are ligands for the SH3, WW, and EVH1 domains, which are present in many synaptic scaffolding, signaling, and cytoskeletal proteins [26]. Therefore, it is possible that PRR7 binds several other synaptic proteins and links them to the NMDA receptor, in order to modulate synaptic plasticity. The proteins that interact with PRR7 should be studied further to understand the roles of PSD in synaptic transmission.

Acknowledgments

We thank Dr. T. Suzuki (Shinshu University) for the preparation of rat forebrain PSD fraction and Dr. H. Togashi (Kyoto University) for rat hippocampal primary culture. pCA-pA plasmid was kindly provided by Drs. H. Niwa and M. Takeichi (RIKEN, Center for Developmental Biology). This work was supported by the Japan New Energy and Industrial Technology Development Organization (NEDO), Grant-in-Aid for Specially Promoted Research (16001005) and JST/CREST (2102014). Y.M. is a Research Fellow of the Japan Society of the Promotion of Science.

References

[1] M.B. Kennedy, Signal-processing machines at the postsynaptic density, Science 290 (2000) 750–754.
[2] M. Sheng, Molecular organization of the postsynaptic specialization, Proc. Natl. Acad. Sci. USA 98 (2001) 7058–7061.
[3] D.S. Bredt, R.A. Nicoll, AMPA receptor trafficking at excitatory synapses, Neuron 40 (2003) 361–379.
[4] M.D. Ehlers, Activity level controls postsynaptic composition and signaling via the ubiquitin–proteasome system, Nat. Neurosci. 6 (2003) 231–242.
[5] R.S. Walikonis, O.N. Jensen, M. Mann, D.W. Provance Jr., J.A. Mercer, M.B. Kennedy, Identification of proteins in the postsynaptic density fraction by mass spectrometry, J. Neurosci. 20 (2000) 4069–4080.
[6] H. Husi, M.A. Ward, J.S. Choudhary, W.P. Blackstock, S.G. Grant, Proteomic analysis of NMDA receptor-adhesion protein signaling complexes, Nat. Neurosci. 3 (2000) 661–669.
[7] K.W. Li, M.P. Hornshaw, R.C. Van Der Schors, R. Watson, S. Tate, B. Casetta, C.R. Jimenez, Y. Gouwenberg, E.D. Gundelfinger, K.H. Smalla, A.B. Smit, Proteomics analysis of rat brain postsynaptic density. Implications of the diverse protein functional groups for the integration of synaptic physiology, J. Biol. Chem. 279 (2004) 987–1002.
[8] J. Peng, M.J. Kim, D. Cheng, D.M. Duong, S.P. Gygi, M. Sheng, Semiquantitative proteomic analysis of rat forebrain postsynaptic density fractions by mass spectrometry, J. Biol. Chem. 279 (2004) 21003–21011.
[9] R.K. Carlin, D.J. Grab, R.S. Cohen, P. Siekevitz, Isolation and characterization of postsynaptic densities from various brain regions: enrichment of different types of postsynaptic densities, J. Cell Biol. 86 (1980) 831–845.
[10] R.S. Cohen, F. Blomberg, K. Berzins, P. Siekevitz, The structure of postsynaptic densities isolated from dog cerebral cortex. I. Overall morphology and protein composition, J. Cell Biol. 74 (1977) 181–203.
[11] A. Shevchenko, M. Wilm, O. Vorm, M. Mann, Mass spectrometric sequencing of proteins silver-stained polyacrylamide gels, Anal. Chem. 68 (1996) 850–858.
[12] F. Gharahdaghi, C.R. Weinberg, D.A. Meagher, B.S. Imai, S.M. Mische, Mass spectrometric identification of proteins from silver-stained polyacrylamide gel: a method for the removal of silver ions to enhance sensitivity, Electrophoresis 20 (1999) 601–605.
[13] H. Niwa, K. Yamamura, J. Miyazaki, Efficient selection for high-expression transfectants with a novel eukaryotic vector, Gene 108 (1991) 193–199.
[14] F. Imamura, S. Maeda, T. Doi, Y. Fujiyoshi, Ligand binding of the second PDZ domain regulates clustering of PSD-95 with the Kv1.4 potassium channel, J. Biol. Chem. 277 (2002) 3640–3646.
[15] K. Goslin, H. Asumussen, G. Banker, Rat hippocampal neurons in low-density culture, in: Culturing Nerve Cells, MIT Press, Cambridge, MA, 1998, pp. 339–370.
[16] H. Togashi, K. Abe, A. Mizoguchi, K. Takaoka, O. Chisaka, M. Takeichi, Cadherin regulates dendritic spine morphogenesis, Neuron 35 (2002) 77–89.

[17] R.L. Strausberg, E.A. Feingold, L.H. Grouse, J.G. Derge, R.D. Klausner, F.S. Collins, L. Wagner, C.M. Shenmen, G.D. Schuler, S.F. Altschul, B. Zeeberg, K.H. Buetow, C.F. Schaefer, N.K. Bhat, R.F. Hopkins, H. Jordan, T. Moore, S.I. Max, J. Wang, F. Hsieh, L. Diatchenko, K. Marusina, A.A. Farmer, G.M. Rubin, L. Hong, M. Stapleton, M.B. Soares, M.F. Bonaldo, T.L. Casavant, T.E. Scheetz, M.J. Brownstein, T.B. Usdin, S. Toshiyuki, P. Carninci, C. Prange, S.S. Raha, N.A. Loquellano, G.J. Peters, R.D. Abramson, S.J. Mullahy, S.A. Bosak, P.J. McEwan, K.J. McKernan, J.A. Malek, P.H. Gunaratne, S. Richards, K.C. Worley, S. Hale, A.M. Garcia, L.J. Gay, S.W. Hulyk, D.K. Villalon, D.M. Muzny, E.J. Sodergren, X. Lu, R.A. Gibbs, J. Fahey, E. Helton, M. Ketteman, A. Madan, S. Rodrigues, A. Sanchez, M. Whiting, A. Madan, A.C. Young, Y. Shevchenko, G.G. Bouffard, R.W. Blakesley, J.W. Touchman, E.D. Green, M.C. Dickson, A.C. Rodriguez, J. Grimwood, J. Schmutz, R.M. Myers, Y.S. Butterfield, M.I. Krzywinski, U. Skalska, D.E. Smailus, A. Schnerch, J.E. Schein, S.J. Jones, M.A. Marra, Generation and initial analysis of more than 15,000 full-length human and mouse cDNA sequences, Proc. Natl. Acad. Sci. USA 99 (2002) 16899–16903.

[18] R.L. Strausberg, E.A. Feingold, R.D. Klausner, F.S. Collins, The mammalian gene collection, Science 286 (1999) 455–457.

[19] M.B. Dalva, M.A. Takasu, M.Z. Lin, S.M. Shamah, L. Hu, N.W. Gale, M.E. Greenberg, EphB receptors interact with NMDA receptors and regulate excitatory synapse formation, Cell 103 (2000) 945–956.

[20] F.J. Lee, S. Xue, L. Pei, B. Vukusic, N. Chery, Y. Wang, Y.T. Wang, H.B. Niznik, X.M. Yu, F. Liu, Dual regulation of NMDA receptor functions by direct protein–protein interactions with the dopamine D1 receptor, Cell 111 (2002) 219–230.

[21] G. Krapivinsky, L. Krapivinsky, Y. Manasian, A. Ivanov, R. Tyzio, C. Pellegrino, Y. Ben-Ari, D.E. Clapham, I. Medina, The NMDA receptor is coupled to the ERK pathway by a direct interaction between NR2B and RasGRF1, Neuron 40 (2003) 775–784.

[22] E. Kim, M. Sheng, PDZ domain proteins of synapses, Nat. Rev. Neurosci. 5 (2004) 771–781.

[23] W. Zhang, L. Vazquez, M. Apperson, M.B. Kennedy, Citron binds to PSD-95 at glutamatergic synapses on inhibitory neurons in the hippocampus, J. Neurosci. 19 (1999) 96–108.

[24] M. Niethammer, J.G. Valtschanoff, T.M. Kapoor, D.W. Allison, T.M. Weinberg, A.M. Craig, M. Sheng, CRIPT, a novel postsynaptic protein that binds to the third PDZ domain of PSD-95/SAP90, Neuron 20 (1998) 693–707.

[25] M. Irie, Y. Hata, M. Takeuchi, K. Ichtchenko, A. Toyoda, K. Hirao, Y. Takai, T.W. Rosahl, T.C. Sudhof, Binding of neuroligins to PSD-95, Science 277 (1997) 1511–1515.

[26] B.K. Kay, M.P. Williamson, M. Sudol, The importance of being proline: the interaction of proline-rich motifs in signaling proteins with their cognate domains, FASEB J. 14 (2000) 231–241.